

C39

Laminar Flow Across Tandem-Manipulated Surface Cylinders: Effect of Reynolds Number and Groove Location

Yousef Gharbia, PhD

Javad Farrokhi Derakhshandeh, PhD

Ibrahim Elbadawy, PhD

ABSTRACT

Controlling the flow between two tandem circular cylinders is a key issue in many engineering applications. This article presents numerical investigations of laminar flow regimes (Re between 50 and 200) over two tandem cylinders. A groove was created on the surface of the upstream cylinder, leaving the downstream cylinder with a smooth surface. The effect of the groove orientation angle with respect to the stagnation point was investigated. The results indicated that the pressure and consequently the imposed forces on the cylinders' surface alter due to the alteration of the wake between and aft the two cylinders as a consequence of the groove orientation. A significant change is found for the lift and drag coefficients of the cylinders. Furthermore, it is found that as Re increases, three distinguished flow regimes known as reattachment flow ($Re = 50$ to 75), transition flow ($Re = 75$ to 100), and coshedding flow ($Re = 100$ to 200), are formed for the two tandem cylinders as a result of the groove.

INTRODUCTION

Flow across tandem cylinders has many engineering applications such as the flow across cooling towers, chimney stacks, subsea pipelines, and capacitors in electronic circuits, etc. Finding ways to manipulate such a flow can lead to altering the imposed pressure on the cylinders, the induced noise, the heat transfer rates, and the wake-induced vibrations. Many numerical and experimental investigations have been conducted to study the characteristics of the flow over single cylinders (Bearman & Zdravkovich, 1978; Bloor, 1964; Kirkgoz et al., 2009) and tandem cylinders (Derakhshandeh et al., 2022; İlkentapar et al., 2023).

Many researchers have been trying to develop innovative techniques to modify the flow across tandem cylinders for various reasons. Kirkgoz et al., 2009 carried out an experimental study on two tandem cylinders mimicking subsea pipelines. They were particularly interested in examining the effect of introducing a spoiler on the upstream and downstream cylinders on the induced oscillations and pressure distribution on the cylinders as well as the resulting vortex structure. Similarly, Hu et al., 2019 simulated the scouring process around two oil pipelines in tandem in a seabed using CFD and the discrete element method (DEM). The study was carried out by varying the stream velocity and the gap ratio (G/D). The results showed that the scour depths below the pipelines are highly dependent on the stream velocity.

Afgan et al., 2023 have conducted a numerical investigation of cross-flow over two heated tandem cylinders using Large Eddy Simulations (LES). The study was conducted at a Reynolds number of 3,000 while varying the cylinder gap ratio between $1.0 \leq L/D \leq 5.0$. Depending on the spacing ratio, the results showed that three main flow regimes were identified: extended-body, reattachment, and co-shedding. Cheng et al., 2023 numerically investigated noise suppression and force oscillations as a result of flow past single and tandem cylinders at a fixed Reynolds number $Re = 12,000$. Similar work was conducted by

Dr. Javad Farrokhi, Ph.D. is associate professor in the Department of Mechanical Engineering, American University of the Middle East, Kuwait. **Dr. Yousef Gharbia, Ph.D.** is associate professor in the Department of Mechanical Engineering, American University of the Middle East, Kuwait. **Dr. Ibrahim Elbadawy, Ph.D.** is assistant professor in the Department of Mechanical Engineering, American University of the Middle East, Kuwait.

Derakhshandeh et al., 2022 on single and two tandem cylinders. The upstream cylinder had a square groove whereas the downstream cylinder and the single cylinders had smooth surfaces. Their investigation was performed at $Re \leq 200$, and groove orientation of 0° , 45° , and 90° with respect to the stagnation point. The gap ratio was kept constant at 4 throughout. The results showed enhancement of the lift force by about 45% and about 20% reduction in drag in comparison with tandem smooth cylinders. Sikdar et al., 2023 numerically studied the effectiveness of using the splitter plate technique in controlling the unsteady flow over a pair of circular cylinders in a tandem arrangement at $Re = 100$ and gap ratio (G/D) between 2 to 5. Ding et al., 2023 studied the induced vibration resulting from the crossflow over two tandem cylinders with different natural frequencies. The investigation was performed using two-dimensional Unsteady Reynolds-Averaged Navier-Stokes equations at Reynolds numbers in the range of $30,000 \leq Re \leq 120,000$ and a gap ratio (G/D) of 2.57. The results showed that the different natural frequencies of the cylinders suppress the vibration of the downstream cylinder.

Maryami et al., 2022 conducted experimental investigation to study the pressure loading on two tandem cylinders subjected to crossflow at Reynolds number of $Re = 30 \times 10^3$ calculated based on the characteristic diameter of the cylinder. The experiments were carried out at difference gap ratio (G/D) ranging between 1.2 to 6. Mousavisani et al., 2022 conducted flow-induced vibration (FIV) experiments on two identical air-inflated flexible circular cylinders in tandem arrangement. The experiments were conducted in a subsonic wind tunnel at Reynolds number in the range of 2, 570–24, 536. The two cylinders of $D = 6$ mm were fixed at their both ends and completely immersed in the flow. The G/D gap ratio was varied between 3 to 7. The FIV responses of the tandem cylinders were compared to those of a similar single cylinder. The results revealed that while the FIV response of the single cylinder exhibited mostly mono-frequency excitation, the FIV response for the tandem cylinders was mainly multi-frequency oscillations.

The primary objective of this research is to address the existing knowledge gap in the field, with a specific focus on enhancing our understanding of the dynamic forces induced by in-phase and anti-phase vortices. The investigation was conducted on tandem cylinders at low Reynolds numbers, in which the Re varies from 75 to 200, aiming to provide valuable insights into how to control the flow over tandem bluff bodies.

NUMERICAL SIMULATION

The model depicts a laminar flow regime across two circular cylinders arranged in tandem within the computational domain. The cylinders have equal diameter, but the leading edge of the upstream cylinder is equipped with a square groove. The basis of the coordinate system is located at the centre of the grooved cylinder, and the spacing ratio between the cylinders is set at $L^* = L/D = 4$. The detail of model and boundary conditions are shown in Figure 1. It is worth noting that a square groove with a length ratio of $T/H = 1$ and a depth to diameter ratio of $H/D = 0.1$ is positioned on the leading surface of the upstream cylinder. The groove is placed at three different angles relative to the front stagnation point, namely $\theta = 0^\circ$, 45° , and 90° . In addition, the domain of the boundary was designed according to the conducted studies in the literature (Alam et al., 2018 and Zhang et al., 2022) to avoid any blockage effects.

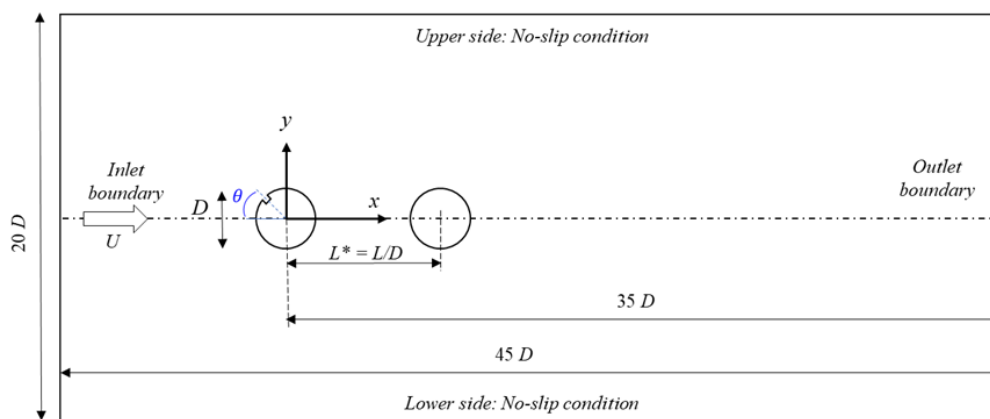


Figure 1 Numerical domain showing the boundary conditions and dimensions.

Mesh structure and quality analysis

In order to ensure the attainment of mesh convergence, an investigation was carried out on three distinct types of mesh structure, namely MS1, MS2, and MS3. Various resolutions were tested for the flow of a single plain cylinder at Reynolds numbers of 200, as indicated in Table 1. The minimum mesh size was determined based on the results of the investigation, and a relatively small-time step of 0.025 seconds was subsequently chosen for laminar flow, in order to satisfy the Courant number condition of $CFL = u\Delta t/\Delta x \leq 1$. The analysis showed that the variations in drag and lift coefficients between different mesh grids were minimal, with a negligible difference of 2%. As a result, it can be concluded that this number of the grid is sufficient to meet the convergence criteria, and therefore, MS2 grid elements was considered to be used for the rest of simulations. A sample of mesh type is shown in Figure 2 around two tandem grooved cylinders.

Table 1. Evaluation of mesh refinement sensitivity for smooth circular cylinders at Reynolds numbers of 200.

Mesh Structure	C_D	C_L	St
MS1 (24,500)	1.31	0.49	0.194
MS2 (455,00)	1.34	0.50	0.202
MS3 (80,000)	1.35	0.50	0.202

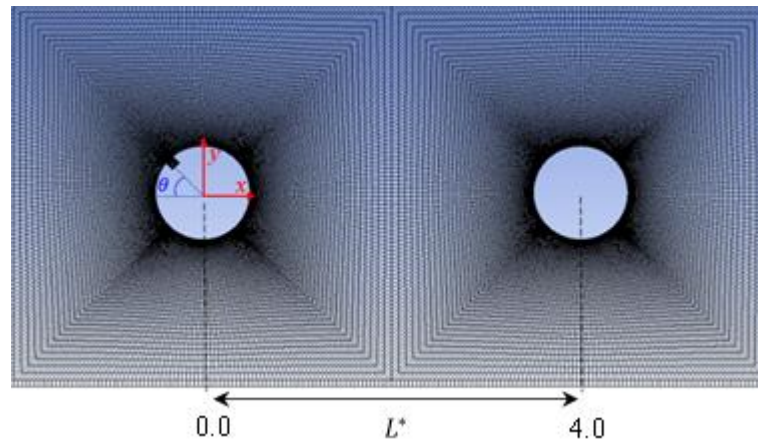


Figure 2 The structured mesh elements surrounding two tandem grooved cylinders are depicted in the figure, with the upstream grooved cylinder oriented at 45 degrees and the gap ratio between the centers indicated.

Verification of the numerical results

The accuracy of the model was checked by simulating the flow over two types of models: i) flow over a single cylinder; ii) flow over two tandem plain circular cylinder and comparing the results to published data (Tables 2 and 3). The numerical results for the single-cylinder case using MS2 were compared to previously published data at $Re = 200$. Table 2 shows a close agreement between the present study and previous published data. For two tandem circular cylinders, upon comparison (see Table 3), it was determined that the results obtained from the numerical simulation closely corresponded to those reported by scholars, indicating a high degree of agreement between the two sets of findings.

Table 2. Comparison of the numerical results, including the average drag coefficient, the lift coefficient fluctuations, and the Strouhal numbers of a single smooth cylinder at $Re = 200$.

Studies	C_D	C_L	St
(Liu et al., 1997)	1.320	NA	0.195
(Singha & Sinhamahapatra, 2010)	1.340	NA	0.195
(Alam, 2016)	1.400	0.498	0.195
(Derakhshandeh & Gharib, 2021)	1.310	0.565	0.198
Present study	1.340	0.501	0.202

Table 3. Comparison of the numerical results, including the lift coefficients of the upstream and downstream cylinders and Strouhal number at $Re = 200$.

References	C_{L1}	C_{L2}	St
(Koda & Lien, 2013)	0.558	1.229	0.170
(Alam, 2016)	0.551	1.117	0.175
Present study	0.559	1.385	0.189

RESULTS AND DISCUSSIONS

Effects of the groove location on the imposed forces and vortex frequency

In Figure 3, at three selected Reynolds number (e.g., $Re = 75, 100,$ and 200), the lift (C_L) and drag (C_D) coefficients' time series are presented for the upstream grooved cylinder at $\theta = 0^\circ$ and the smooth downstream cylinder (left and middle columns, respectively), which are denoted by Figure 3 $a_1 - a_3$, and Figure 3 $b_1 - b_3$). This graphical representation provides a comparative analysis of the two types of cylinders' coefficient behaviors, allowing for a better understanding of their performance characteristics. The power spectral densities of the lift coefficients are also shown in the right column (Figure 3 $c_1 - c_3$).

The results of the PSD show that each power spectrum manifests a prevailing value of St that corresponds to the non-dimensional frequency of vortex shedding. By increasing the Reynolds number, the primary vortex shedding frequency gradually increases, leading to a more discernible PSD peak. Notably, the St number, which corresponds to the location of the PSD peak, approaches approximately 0.2 at $Re = 200$, which is consistent with the vortex shedding frequency of a single cylinder in literature. Upon comparing the PSD results, it is evident that the frequency of vortex shedding experiences a surge of up to 60% as the Reynolds number (Re) changes from 75 to 200.

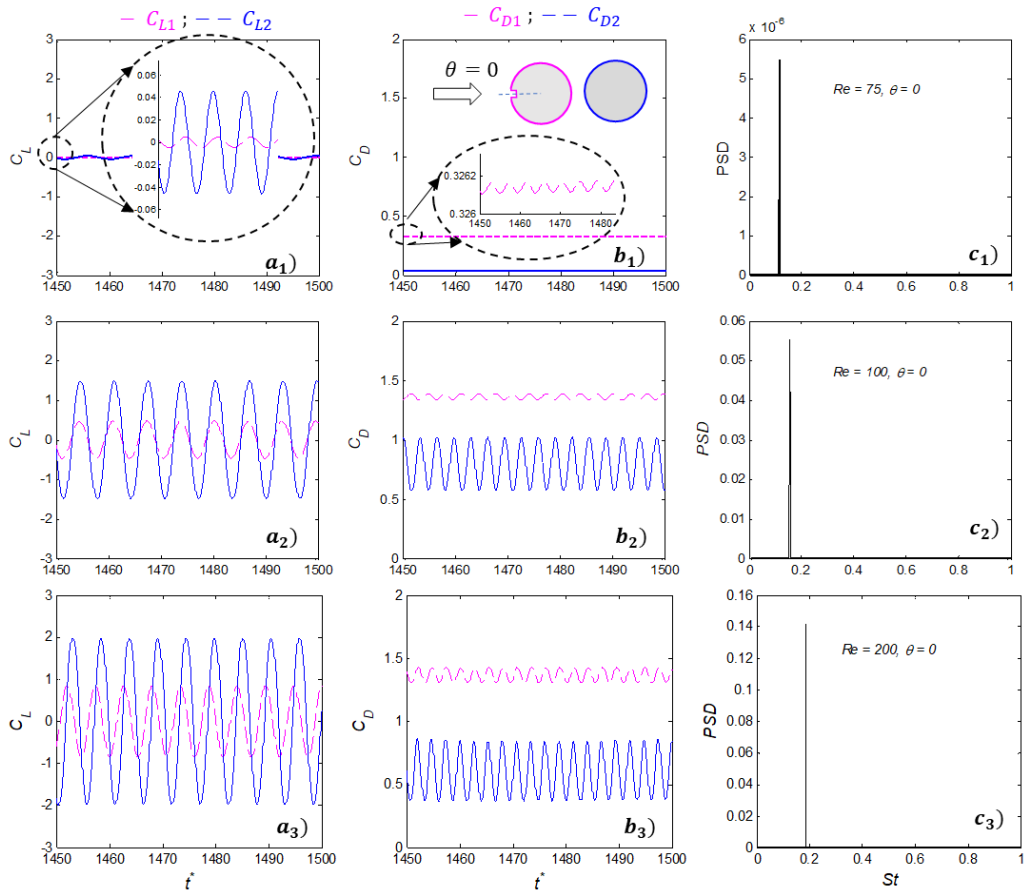


Figure 3 Samples of lift and drag coefficients at selected Re (left and middle column) and power spectral density of the lift coefficient showing the Strouhal Numbers (right column).

Effects of the groove location on the vorticity

The vorticity contours in the spanwise direction (ω^*) for a pair of tandem-grooved cylinders are depicted in Figure 4. The Reynolds numbers analyzed were 75, 100, 125, and 200. The upstream cylinder was equipped with a single square-shaped groove situated at $\theta = 0^\circ$, 45° , and 90° , whereas the downstream cylinder remained ungrooved. It is observed that at a $Re = 75$, the free shear layers separated from the upstream cylinder for all the examined angles and then reattached to the downstream cylinder. This reattachment induced the creation of vortices around the downstream cylinder. Under the reattachment flow (RF) regime, the flow between two cylinders exhibited nearly symmetrical behavior.

For larger Reynolds number, e.g., $Re \geq 100$, the flow between the cylinders exhibited primary vortices (positive and negative), known as the co-shedding flow (CF) regime. In this regime, the effect of θ on the vortex feature in the gap became more significant compared to the RF regime ($Re = 75$). The wake structure of the downstream cylinder was also different from that of $\theta \leq 0^\circ$ at $Re = 75$. The phase lag and vortex pattern relationship varied between the flow regimes. In the CF regime, the shedding was anti-phase for all test cases, and primary vortices were placed closer to the downstream cylinder, accompanied by secondary vortices, forming a secondary Von Karman Street. As Re increased more, the gap vortices, binary vortex, and secondary vortices in the downstream cylinder wake became stronger. The spacing between positive and negative vortices, thus, decreased with the increase of Re . The contour plots also demonstrate that the spacing of the primary and secondary vortices in the wake of the downstream cylinder was sensitive to Re , especially for $Re = 125$ and 200. Therefore, it has been determined that the Reynolds number and the placement of the groove on the upstream cylinder's leading surface are crucial

factors in controlling the flow between and behind the tandem cylinders. This, in turn, can modify the applied forces on the cylinders' surfaces, which is a crucial concept in the field of aerodynamics.

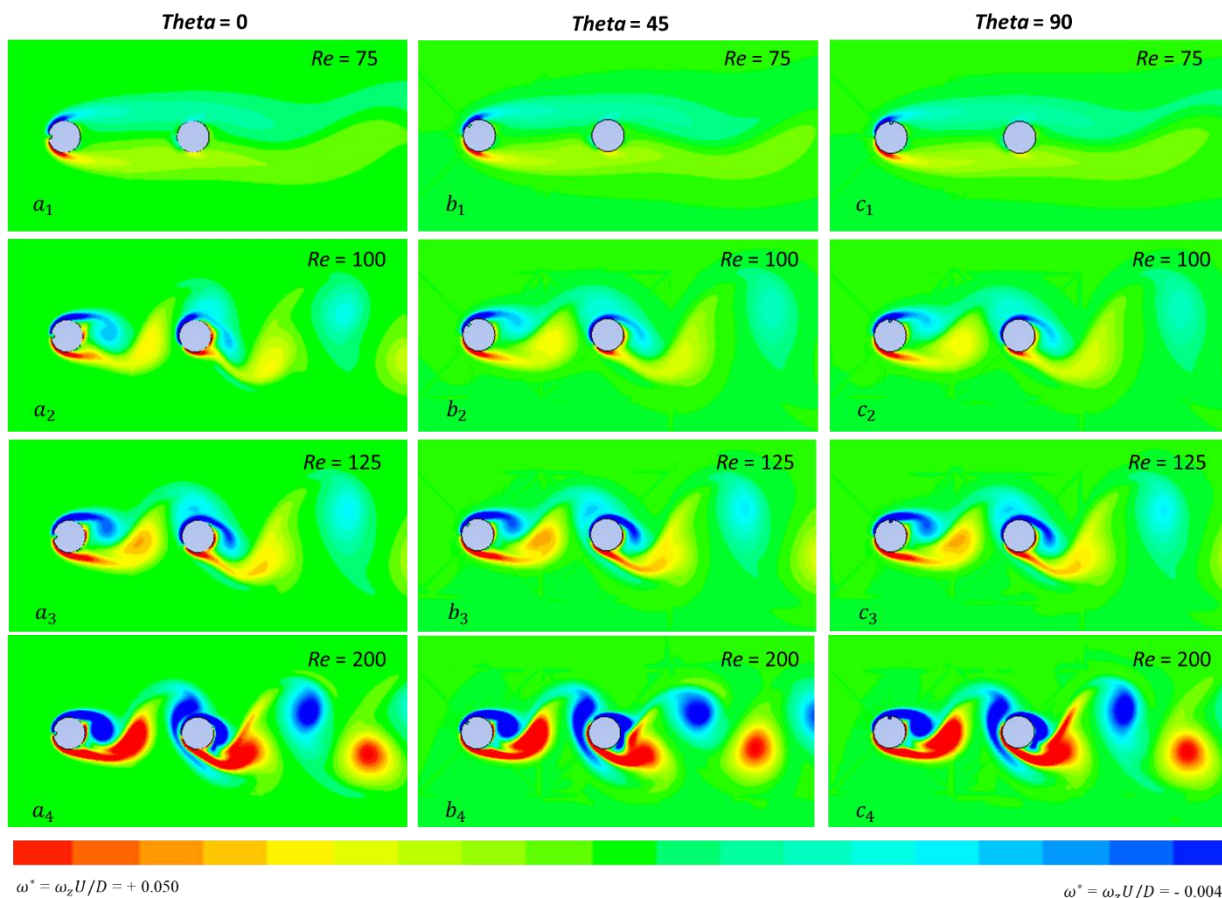


Figure 4 Vorticity contours for selected $Re = 75, 100, 125$ and 200 once the location angle of the groove changes on the leading surface of the upstream cylinder.

CONCLUSIONS

Numerical simulations were conducted to examine the effect of Reynolds number ($Re = 50-200$) on the flow over two tandem grooved cylinders once the gap ratio of the cylinder was set at $L^* = 4$. The study conducted simulations to extract important parameters, such as lift and drag coefficients, Strouhal number (St), and vorticities. The obtained data were thoroughly analyzed and discussed in the research. It can be concluded that the flow control between and behind the tandem cylinders is heavily influenced by the Reynolds number and the location of the groove on the leading surface of the upstream cylinder. These factors can result in alterations to the applied forces on the cylinder surfaces, which are critical considerations in the field of aerodynamics and hydrodynamics. It was found that, a noticeable increase of up to 60% in the frequency of vortex shedding was observed as the Reynolds number (Re) increased from 75 to 200. This concept of vortex shedding frequency should be considered in terms of resonance phenomenon in several fields such as mechanical, civil and aerodynamics applications.

REFERENCES

- Afgan, I., Kahil, Y., Benhamadouche, S., Ali, M., Alkaabi, A., Sofiane Berrouk, A., & Sagaut, P. (2023). Cross flow over two heated cylinders in tandem arrangements at subcritical Reynolds number using large eddy simulations. *International Journal of Heat and Fluid Flow*, 100(January), 109115. <https://doi.org/10.1016/j.ijheatfluidflow.2023.109115>
- Alam, M. M. (2016). Lift forces induced by phase lag between the vortex sheddings from two tandem bluff bodies. *Journal of Fluids and Structures*, 65, 217–237. <https://doi.org/10.1016/j.jfluidstructs.2016.05.008>
- Alam, M. M., Zheng, Q., Derakhshandeh, J. F., Rehman, S., Ji, C., & Zafar, F. (2018). On forces and phase lags between vortex sheddings from three tandem cylinders. *International Journal of Heat and Fluid Flow*, 69(May 2017), 117–135. <https://doi.org/10.1016/j.ijheatfluidflow.2017.12.012>
- Bearman, P. W., & Zdravkovich, M. M. (1978). Flow around a circular cylinder near a plane boundary. *Journal of Fluid Mechanics*, 89(1), 33–47. <https://doi.org/10.1017/S002211207800244X>
- Bloor, M. S. (1964). The transition to turbulence in the wake of a circular cylinder. *Journal of Fluid Mechanics*, 19(2), 290–304. <https://doi.org/10.1017/S0022112064000726>
- Cheng, Z., McConkey, R., Yee, E., & Lien, F. S. (2023). Numerical investigation of noise suppression and amplification in forced oscillations of single and tandem cylinders in high Reynolds number turbulent flows. *Applied Mathematical Modelling*, 117, 652–686. <https://doi.org/10.1016/j.apm.2023.01.004>
- Derakhshandeh, J. F., Gharbia, Y., & Ji, C. (2022). Numerical investigations on flow over tandem grooved cylinders. *Ocean Engineering*, 251(December 2021), 111160. <https://doi.org/10.1016/j.oceaneng.2022.111160>
- Derakhshandeh, J. F., & Gharib, N. (2021). Numerical studies of laminar flow over two tandem elliptical cylinders using Ramanujan approximation. *Journal of the Brazilian Society of Mechanical Sciences and Engineering*, 43(3). <https://doi.org/10.1007/s40430-021-02890-0>
- Ding, W., Chai, Y., Liu, H., Zhang, G., & Mao, Z. (2023). Numerical investigation on flow-induced vibrations of two tandem cylinders localized selective roughness with different natural frequencies. *Applied Ocean Research*, 135(February), 103540. <https://doi.org/10.1016/j.apor.2023.103540>
- Hu, D., Tang, W., Sun, L., Li, F., Ji, X., & Duan, Z. (2019). Numerical simulation of local scour around two pipelines in tandem using CFD–DEM method. *Applied Ocean Research*, 93(April). <https://doi.org/10.1016/j.apor.2019.101968>
- İlkentapar, M., Akşit, S., Açikel, H. H., & Öner, A. A. (2023). The effect of spoilers on flow around tandem circular cylinders. *Ocean Engineering*, 272(January), 113637. <https://doi.org/10.1016/j.oceaneng.2023.113637>
- Kirkgoz, M. S., Oner, A. A., & Aköz, M. S. (2009). Numerical modeling of interaction of a current with a circular cylinder near a rigid bed. *Advances in Engineering Software*, 40(11), 1191–1199. <https://doi.org/10.1016/J.ADVENGSOFT.2009.03.019>
- Koda, Y., & Lien, F. S. (2013). Aerodynamic effects of the early three-dimensional instabilities in the flow over one and two circular cylinders in tandem predicted by the lattice Boltzmann method. *Computers and Fluids*, 74, 32–43. <https://doi.org/10.1016/j.compfluid.2013.01.003>
- Liu, C., Zheng, X., Liao, C., Sung, C. H., & Huang, T. T. (1997). Preconditioned multigrid methods for unsteady incompressible flows. *35th Aerospace Sciences Meeting and Exhibit, January*. <https://doi.org/10.2514/6.1997-445>
- Maryami, R., Ali, S. A. S., Azarpeyvand, M., Dehghan, A. A., & Afshari, A. (2022). The influence of cylinders in tandem arrangement on unsteady aerodynamic loads. *Experimental Thermal and Fluid Science*, 139(April 2021), 110709. <https://doi.org/10.1016/j.expthermflusci.2022.110709>
- Mousavisani, S., Castro, G., & Seyed-Aghazadeh, B. (2022). Experimental investigation on flow-induced vibration of two high mass-ratio flexible cylinders in tandem arrangement. *Journal of Fluids and Structures*, 113, 103640. <https://doi.org/10.1016/j.jfluidstructs.2022.103640>
- Sikdar, P., Dash, S. M., & Sinhamahapatra, K. P. (2023). A numerical study on the drag reduction and wake regime control of the tandem circular cylinders using splitter plates. *Journal of Computational Science*, 66, 101927. <https://doi.org/10.1016/J.JOCS.2022.101927>
- Singha, S., & Sinhamahapatra, K. P. (2010). High-Resolution numerical simulation of low Reynolds number incompressible flow about two cylinders in tandem. *Journal of Fluids Engineering, Transactions of the ASME*, 132(1), 0111011–01110110. <https://doi.org/10.1115/1.4000649>
- Zhang, Z., Ji, C., Xu, D., Zhu, H., Derakhshandeh, J. F., & Chen, W. (2022). Effect of yaw angle on vibration mode transition and wake structure of a near-wall flexible cylinder. *Physics of Fluids*, 34(7). <https://doi.org/10.1063/5.0096149>